

Text-driven Editing of 3D Scenes without Retraining

Shuangkang Fang¹ Yufeng Wang¹ Yi Yang²
Yi-Hsuan Tsai³ Wenrui Ding¹ Ming-Hsuan Yang^{3,4,5} Shuchang Zhou²
¹Beihang University ²Megvii ³Google
⁴University of California, Merced ⁵Yonsei University

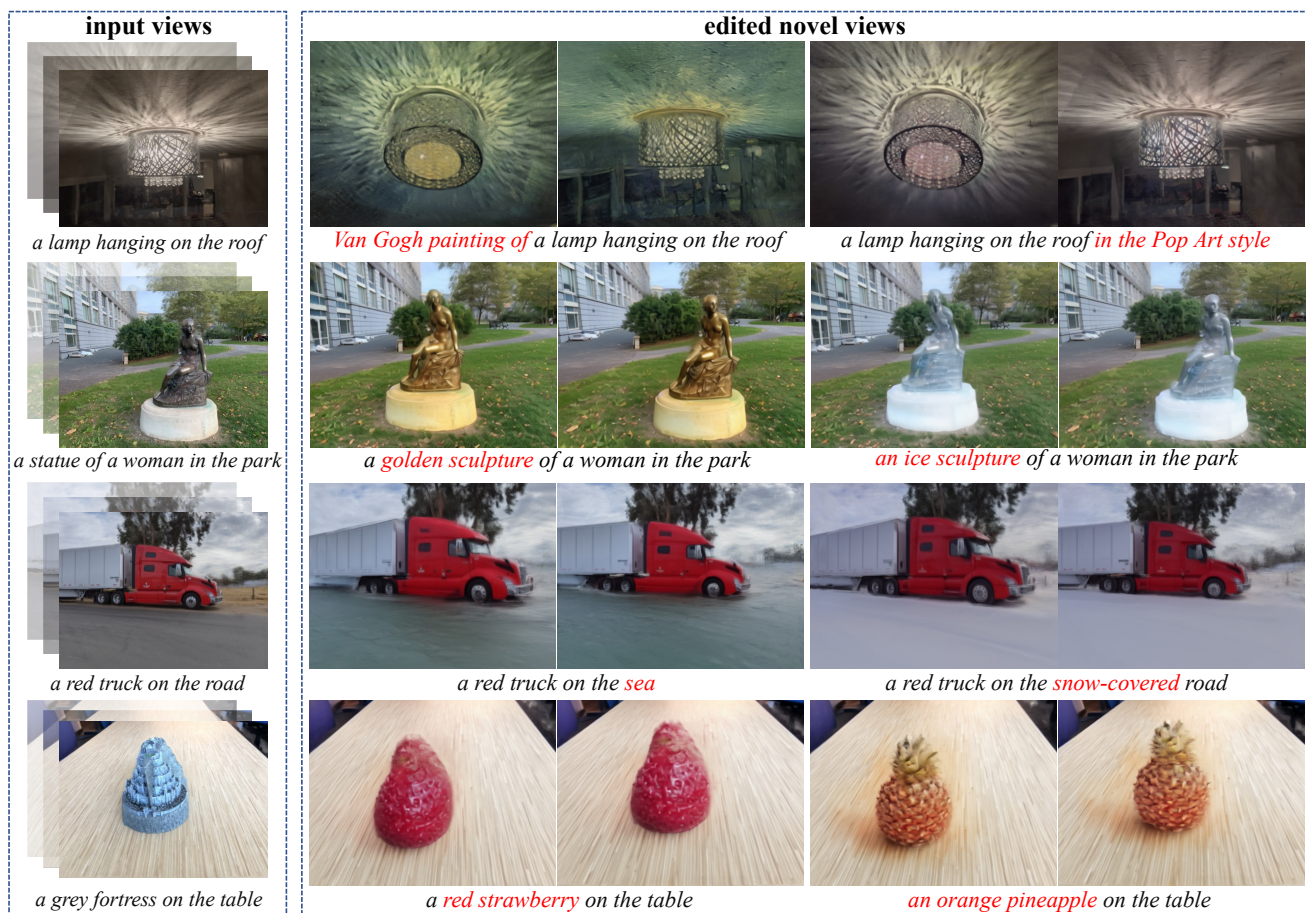


Figure 1. **Visualization results of our method in 3D scene editing.** The proposed DN2N method enables users to obtain realistic and 3D consistent novel views that correspond to the target caption without retraining a new model.

Abstract

Numerous diffusion models have recently been applied to image synthesis and editing. However, editing 3D scenes is still in its early stages. It poses various challenges, such as the requirement to design specific methods for different editing types, retraining new models for various 3D scenes,

and the absence of convenient human interaction during editing. To tackle these issues, we introduce a text-driven editing method, termed DN2N, which allows for the direct acquisition of a NeRF model with universal editing capabilities, eliminating the requirement for retraining. Our method employs off-the-shelf text-based editing models of 2D images to modify the 3D scene images, followed by a

filtering process to discard poorly edited images that disrupt 3D consistency. We then consider the remaining inconsistency as a problem of removing noise perturbation, which can be solved by generating training data with similar perturbation characteristics for training. We further propose cross-view regularization terms to help the generalized NeRF model mitigate these perturbations. Our text-driven method allows users to edit a 3D scene with their desired description, which is more friendly, intuitive, and practical than prior works. Empirical results show that our method achieves multiple editing types, including but not limited to appearance editing, weather transition, material changing, and style transfer. Most importantly, our method generalizes well with editing abilities shared among a set of model parameters without requiring a customized editing model for some specific scenes, thus inferring novel views with editing effects directly from user input. The project website is available at <http://sk-fun.fun/DN2N>.

1. Introduction

Significant advances of neural radiance field (NeRF) techniques [1, 9, 14, 15, 38, 39, 44, 48, 66–68] have been modeled for a variety of vision tasks including novel view synthesis and editing. Numerous NeRF-based methods have been developed to achieve specific types of 3D manipulating, such as the color editing [33, 41, 64], scene composition [61, 62], weather transformation [36], multiple editing [14, 15], and style transfer [18, 25, 28]. Recently, a few attempts have been made to leverage multi-modal techniques to design text-guided 3D editing methods [20, 69]. Despite the demonstrated success, there remain several challenges. 1) existing methods typically rely on known editing types in advance, resulting in limited modification capabilities; 2) retraining an editing model is required for each particular 3D scene, leading to computational and memory overhead; 3) these editing techniques are often less user-friendly.

In this work, we propose a novel 3D scene editing method to tackle the aforementioned challenges. The main objective is to construct a more accessible, user-friendly, and convenient editing process that enables experts and novices to achieve diverse scene edits through imaginative and creative approaches. The development of controllable 2D image editing techniques [5, 12, 22, 24, 45, 53, 56, 58] makes it possible to achieve this objective. We consider designing a text-driven and generalized method that involves editing the images of a 3D scene using the off-the-shelf 2D image editing models, followed by reconstructing the edited scene using a generalizable NeRF model. Nonetheless, creating such an editing pipeline presents several challenges. For example, applying 2D-image editing directly makes it challenging to achieve 3D consistency, and the degree of 3D

inconsistency may vary depending on the scene and editing type. Furthermore, creating a generalized model that does not require retraining for different scenes and editing types necessitates abundant task-specific 3D scene data.

To address the aforementioned issues, we initially utilize a 2D editing model to perform the preliminary editing on the images of a 3D scene. We subsequently apply a designed content filter to remove images with poor editing results that cause significant 3D inconsistency. However, the remaining images after selection may still contain inconsistent 3D results, in which we consider as noise perturbation to the consistent edited images due to the inherent stochastic and diverse nature of the 2D editing model. Thus, we leverage this characteristic to create training data pairs by generating image captions through the BLIP model [34, 35] and target captions via GPT [6], then applying minor perturbations associated with these captions to a 3D scene. Therefore, these perturbations can be viewed as noise, as well as unedited images as pseudo ground truth (see the left part of Figure 2(a)). Based on this produced training data, we introduce two cross-view regularization terms during training, including the self and neighboring views, to improve the 3D editing consistency. The former requires the NeRF model to generate consistent results for the same target view that derives from two different source views, while the latter enforces the overlapping pixel values between the target and adjacent views to be approximately close. Finally, both the perturbation dataset and regularization terms are incorporated into our generalizable NeRF model training to facilitate its 3D consistency.

The main contributions of this work are:

- We propose a versatile text-driven method for editing 3D scenes, capable of synthesizing novel views to match a given textual description while preserving 3D consistency without customizing or retraining a model for different scenes and editing types.
- We develop a new 3D scene editing framework named DN2N that employs off-the-shelf 2D editing models for 3D scene manipulation, where the induced 3D inconsistency is modeled as noise perturbation and addressed by generating training data with similar perturbation characteristics for optimization.
- We design a generalizable NeRF model architecture and integrate cross-view regularization terms into the training process to enhance the 3D consistency in edited novel views.
- We conduct extensive experiments of different editing types on multiple datasets. Compared with other methods, our model not only produces consistent 3D scenes but also offers generality and diverse editing capabilities.

2. Related work

NeRF-based novel view synthesis. Novel view synthesis based on NeRF has recently gained significant attention in the vision and graphics communities [9, 15, 17, 38, 44, 48, 67]. NeRF represents the structure and appearance of a 3D scene by using a neural network that takes the spatial location and view direction as input and outputs the corresponding color and opacity at each pixel. Subsequent works have improved NeRF, such as speeding up the training process [9, 48, 62], designing better sampling strategies [1], and enhancing generalization ability [8, 29, 40, 66].

Diffusion-based image editing. Diffusion-based models have been widely used in image generation [11, 12, 24, 52, 53, 56–59]. In addition, numerous text-based image editing methods such as GLIDE [49] and Stable Diffusion [53] have recently been developed. Imagic [30] fine-tunes images according to text descriptions, and Prompt-to-prompt [22] preserves unedited regions by utilizing cross-attention information, enabling controlled image editing. On the other hand, Pix2pix-zero [50] employs a set of embedding vector mechanisms to establish controllable editing directions for images. In [5], InstructPix2Pix trains a model by generating a large number of text-editing image pairs using GPT [7] and Stable Diffusion [53]. Null-text inversion [45] proposes a more accurate diffusion inversion process to enhance image-controlled editing capabilities.

3D scene editing. Numerous 3D scene editing approaches have been developed based on point cloud representations [27, 46], and scene texture mapping based on triangle meshes [2, 19, 25, 70]. However, these methods are limited by the inherent scene representations, which restrict scalability and editing capability. Recently, NeRF has been used for 3D scene editing in numerous approaches, including appearance editing [3, 4, 33, 37, 55, 63], scene combining [17, 62], weather simulation [36, 60], assemble editing [14, 15], and style transfer [10, 18, 26, 28, 42, 47, 65, 69]. However, several aspects of existing 3D editing methods based on NeRF are limited. For instance, they are usually restricted to performing a single editing task, necessitating separate model structures and training approaches for each editing capability. To overcome this limitation, PVD-AL [15] employs distillation to achieve multiple editing capabilities in one model, although with lower efficiency. Instruct-NeRF2NeRF [20] enables controllable editing of 3D scenes by pre-editing 2D images using InstructPix2Pix [5]. However, Instruct-NeRF2NeRF has two notable drawbacks. First, retraining is necessary for each new editing direction, resulting in significant computation and memory overhead. Second, the method generates new training data and updates model parameters during training, which is time-consuming and unsuitable for interactive editing. In contrast, our method overcomes these two problems by requiring only the target text to obtain the cor-

responding 3D scene editing, using the same model for any editing types without retraining, thereby reducing model storage consumption and training time.

3. Method

Figure 2 shows the overall framework of our method. At the training stage, we first utilize BLIP [35] and GPT [6] models to generate the input caption and target caption of a scene. We then use a 2D image editing model [45] to apply minor editing perturbations to the scene based on these captions to obtain training data pairs, while the training objective of our model is to remove these perturbations (see Eq. 4). We use two sets of independent source views to render the same target view, resulting in Tgt_a and Tgt_b , respectively, and render a neighboring view around the target view to obtain Nbr . Then we impose a consistency loss (see Eq. 5 and Eq. 6) on the three rendered results. At the inference stage, we begin by applying standard magnitude editing to the 3D scene. Subsequently, we filter out images with poor editing effects and those inducing significant disruptions to the 3D consistency (see Eq. 9). Finally, we feed the filtered images into the generalizable NeRF model to obtain edited novel views directly.

Optimization objectives. A 3D scene training data consists of N images and their corresponding camera parameters, including both internal and external parameters: $\{I_i, P_i\}_{i=1}^N$. To obtain the pre-edited image \tilde{I}_i for each I_i , we employ the 2D image editing model, which is defined as:

$$\tilde{I}_i = \mathcal{F}(I_i, C_{in}^i, C_{tgt}^i, \theta), \quad (1)$$

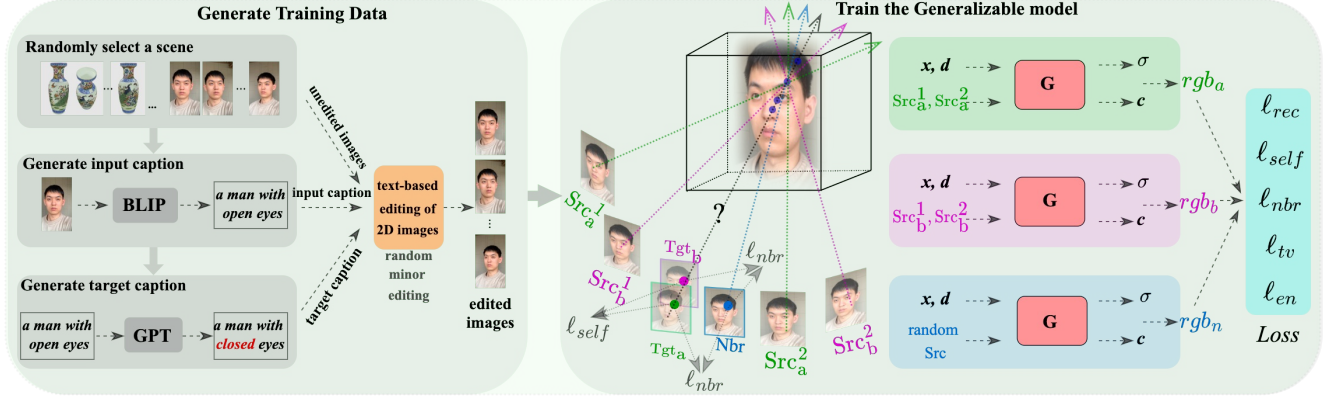
where C_{in}^i is input caption for the unedited image I_i , C_{tgt}^i is target caption for the edited image \tilde{I}_i , and θ is the hyper-parameters of model \mathcal{F} . After filtering out the poorly edited images that disrupt 3D consistency, the resulting data is denoted as $\{\tilde{I}_m, P_m\}_{m=1}^M$, where $M < N$. Then the generalized NeRF model G with parameter Θ predicts the target view \hat{I}_m using K source views $\{\tilde{I}_k, P_k\}_{k=1}^K$:

$$\hat{I}_m = G(\tilde{I}_k, P_k, \Theta \mid k = 1, \dots, K, P_k \neq P_m). \quad (2)$$

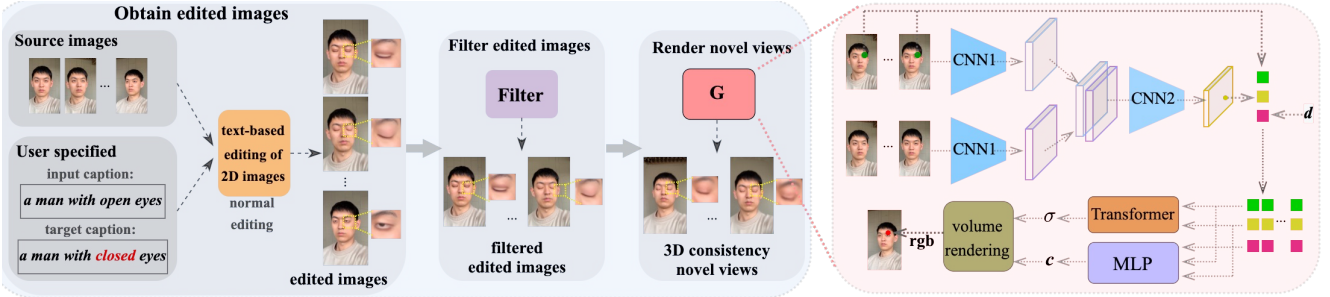
Assuming that the ground truth of edited images with 3D consistency is denoted as \check{I}_m , our optimization objective can be expressed as:

$$\arg \min_{\Theta} \sum_{m=1}^M \left\| \check{I}_m - \hat{I}_m \right\|^2. \quad (3)$$

However, the edited ground truth \check{I}_m is not at our disposal. Thus, we express the result of Eq. 1 as $\tilde{I}_m = \check{I}_m + \Delta I_m$. This implies that the images edited by model \mathcal{F} can be perceived as edited ground truth images with minor perturbations caused by noise. In this work, the perturbations



(a) **Training stage.** We generate training data by applying subtle perturbations to 3D scenes using the BLIP [35], GPT [6], and 2D editing models [45]. Subsequently, we train the DN2N model by incorporating cross-view regularization terms, ℓ_{self} and ℓ_{nbr} , with the generalized NeRF model G .



(b) **Inference stage.** We devise a content filter to eliminate the images with subpar editing results and compromised consistency. Then, we utilize the well-trained model to obtain the edited novel views.

Figure 2. **Illustration of the DN2N framework.** See Sec 3 for the detailed description.

mainly stem from the lack of consistency in the training dataset after 2D image editing by model \mathcal{F} . Hence, we can apply similar random minor perturbations ΔI_i to clean 3D scene images $\{I_i\}_{i=1}^N$ by controlling the parameters θ in \mathcal{F} , resulting in $\{\tilde{I}_i\}_{i=1}^N$. We use the $\{\tilde{I}_i\}_{i=1}^N$ as pseudo ground truth to train the model G . As such, the objective function constructed for model training is:

$$\arg \min_{\Theta} \sum_{i=1}^N \left\| I_i - G(\tilde{I}_k, P_k, \Theta \mid k=1, \dots, K, P_k \neq P_i) \right\|^2. \quad (4)$$

Generate training data. To generate training data pairs, we utilize the off-the-shelf tools BLIP [35] and GPT [6]. As illustrated in Figure 2, we select an image from a scene at random and feed it into the BLIP model to obtain its input caption, such as “a man with open eyes.” Subsequently, we use GPT to generate the target caption, such as “a man with closed eyes.” Additional information and examples regarding the generation process are available in the supplementary material. For each image of a scene, we apply minor perturbations randomly using Eq. 1 by controlling the hyper-parameters θ .

Self-view robustness. We use a training approach similar to that in the generalizable NeRF models [29, 40, 66],

which involves predicting the target view based on several source views. When the training data of a 3D scene is consistent, predicting the same target view with different source views typically yields consistent results. However, this may not hold for the scene pre-edited by a 2D-editing model. To address this, we perform two independent predictions, labeled \mathcal{A} and \mathcal{B} . For \mathcal{A} , we use source views $\{Src_a^1, Src_a^2, \dots\}$ and predict the target view as Tgt_a . Additionally, for \mathcal{B} , we use source views $\{Src_b^1, Src_b^2, \dots\}$ and predict the same target view as Tgt_b . We calculate the L2 loss to ensure consistency between two predictions:

$$\ell_{self} = \|Tgt_a - Tgt_b\|^2. \quad (5)$$

Neighboring view consistency. Empirically, we observe that there are often noticeable texture or color discontinuities between adjacent views when rendering along a smooth camera path. To tackle this issue, we enforce a smooth transition between adjacent views. Specifically, we slightly perturb the pose corresponding to the target view and generate a novel view based on the perturbed pose, which we refer to as the neighboring view Tgt_{nbr} . We project the pixel points from the target view onto the

neighboring view using depth and calculate the following loss to minimize the image discontinuities caused by changes in the viewing angle:

$$\ell_{nbr} = \|M(Tgt_a - Tgt_{nbr})\|^2 + \|M(Tgt_b - Tgt_{nbr})\|^2, \quad (6)$$

where M refers to a mask, which indicates that only the loss between overlapping regions is calculated. In addition, we note that the weights of some sampled points on the rays are distributed along the rays. This can lead to distortions such as floating objects in the predicted target view, and inaccurate depth estimates, which may affect the accuracy of the target view to neighboring view projection. Similar to [31], we introduce an entropy loss for the weights of the sampling points:

$$\ell_{en} = -\sum T_i(1 - \exp(-\sigma_i\delta_i)) \log(T_i(1 - \exp(-\sigma_i\delta_i))), \quad (7)$$

where σ_i is the density of the spatial points sampled along a ray. δ_i denotes the distance between adjacent sample points. Please refer to the Appendix for the definition of T_i and additional details.

Network structure. The generalized NeRF model G in Figure 2 is developed based on the IBRNet [66]. We extend it by incorporating multi-viewpoint aggregation, cross-view mappings, and integration of unedited image information to render consistent results. More details regarding the generalized NeRF model G are described in the supplementary material.

Loss function. During training, the model cannot render a complete image in a single forward pass due to GPU memory limitations. Thus, the model predicts image patches at each training step, and the loss is computed on a patch level. The total loss function employed in this work is:

$$\ell = \ell_{rec} + \lambda_1 \ell_{self} + \lambda_2 \ell_{nbr} + \lambda_3 \ell_{en} + \lambda_4 \ell_{tv}, \quad (8)$$

where $\ell_{rec} = \left\| I_i - \hat{I}_i \right\|^2$ is obtained from Eq. 4, and ℓ_{tv} is the total variation regularization term [54].

Content filter. During the inference phase, we design a content filter to remove poorly edited images and those that cause significant inconsistency. The remaining perturbations caused by 2D editing are then removed using the trained model. Our content filter is designed based on four tuples:

$$\left\{ \text{SSIM}(I_i, \tilde{I}_i), \text{CLIP}(I_i, \tilde{I}_i), \text{CLIP}(\tilde{I}_i, C_{tgt}), \text{CLIP}(I_i, \tilde{I}_i) - \text{CLIP}(C_{in}, C_{tgt}) \right\}_{i=1}^N. \quad (9)$$

We calculate these four groups of values for all the edited images, sort each set of results, and discard the top 10% or

bottom 10% of the data. This content filter significantly reduces the 3D inconsistency among the edited images. More details are presented in the Appendix.

4. Experiments and Analysis

The datasets used to train our model are Google Scanned Objects [13], NeRF-Synthetic [44], Spaces [16] and the IBRNet-collect [66]. The LLFF [43] and NeRF-Art [65] are used for evaluation. The default 2D-image editing model is Null-text [45]. We implement our method with PyTorch [51], train the model on 8 NVIDIA V100 GPUs, and use one single V100 GPU for inference. More implementation details and results are presented in the supplementary material.

4.1. Qualitative results

As illustrated in Figure 1, our approach demonstrates its ability to achieve various challenging editing types without retraining while maintaining 3D consistency and conforming to the text description. More editing results are presented in the supplementary material. To further assess the effectiveness of our approach, we conduct comparative studies against state-of-the-art methods.

Text-driven 3D scene editing. We compare our approach to other text-driven editing methods, as shown in Figure 3. NeRF-Art utilizes multiple loss functions to retrain a model corresponding to given words, with limitations in achieving complex and precise editing effects. Instruct-NeRF2NeRF initially edits 2D images according to instruction and trains a model using these edited images, then generates new images by the model, which are further edited again to train the model iteratively until it produces images that comply with the instructions. In contrast, the scene editing results by our DN2N are directly inferred by the model after the given text without any intervening training process, whereas NeRF-Art and Instruct-NeRF2NeRF require retraining a model for each scene and each editing type. In addition, the editing results by DN2N are more realistic and retain more areas unrelated to the target caption, as shown in Figure 3, making it easier to achieve cascading multiple edits (see the supplementary material for more details).

Style transfer. In Figure 4, we present visual comparisons rendered by DN2N and other 3D scene style transfer techniques. As depicted, the Learning-to-Stylize method tends to imitate the color information of the reference image, but it often overlooks curved strokes. On the other hand, ARF excessively imitates curved strokes of the reference image, resulting in less pleasing visual effects and loss of information in the original scene. In contrast, our approach synthesizes the scenes by capturing both the color and stroke of the target style. Furthermore, both evaluated methods necessitate selecting a reference image first and

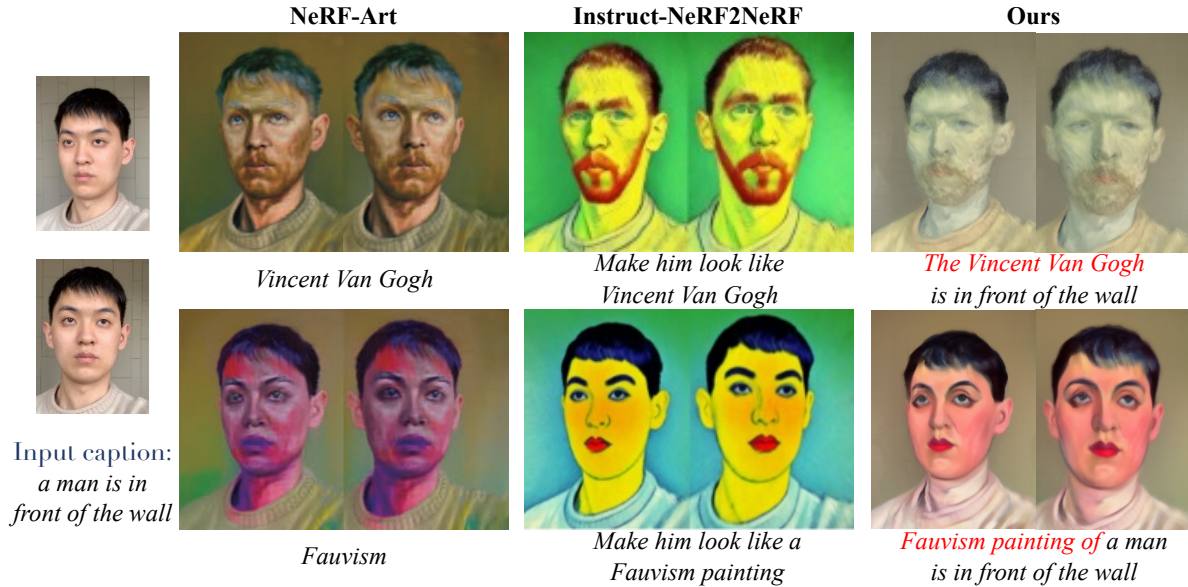


Figure 3. **Comparison with other text-driven editing methods.** DN2N strikes a better balance between preserving image content and aligning with textual descriptions. More importantly, it is not necessary to retrain our model for different editing types.

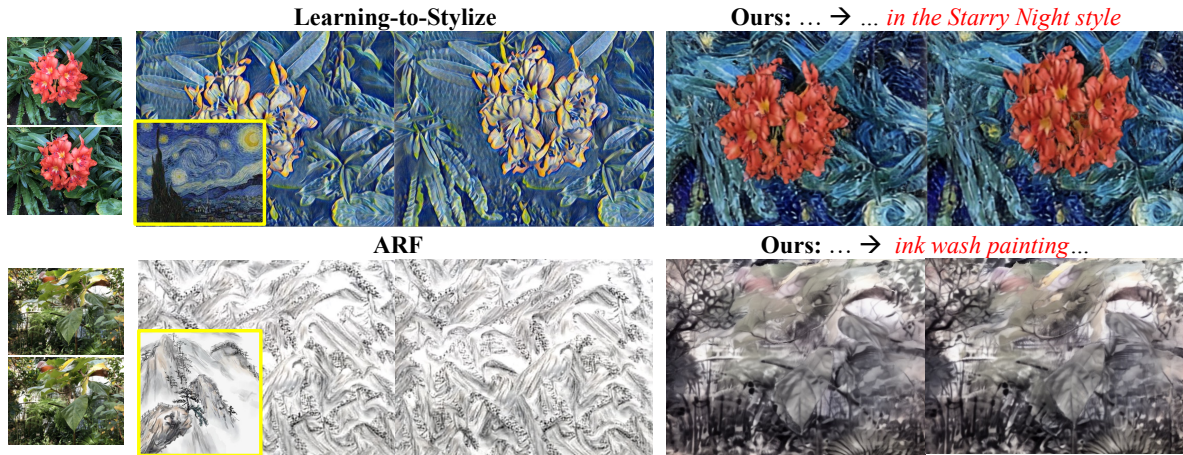


Figure 4. **Comparison with other methods for editing scene styles.** DN2N can more accurately transfer colors and brush strokes while preserving more original image content.

then retraining an editing model whereas our method is text-driven and user-friendly, without the need for retraining. As such, our method reduces training requirements and model storage, thereby offering friendly image editing capabilities.

Appearance editing. Two steps are involved in editing the appearance of an object in a scene: determining the target area and editing the appearance of that area. As illustrated in Figure 5, our method accurately locates the target area and applies appearance editing consistent with the target description without requiring training. While Clip-NeRF uses CLIP Similarity to limit the novel view to the

target words, it is not able to accurately locate the target area or transfer visual appearance. In addition, the area outside the target is also modified. DFF uses DINO or Lseg to inject label information into points in space, ensuring precise editing area localization. However, its appearance editing requires manual operations, such as specifying the RGB value of the editing area. Furthermore, both methods require training separate models for each scene, making them less efficient than DN2N.

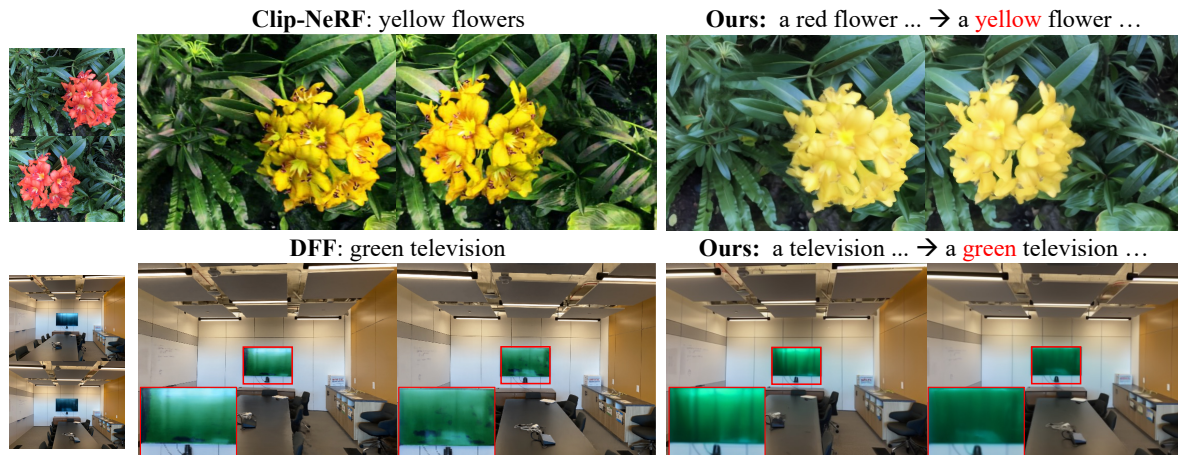


Figure 5. **Comparison with other methods for editing appearance.** DN2N achieves higher accuracy in matching target captions while effectively preserving information in non-edited areas.

4.2. Quantitative results

Ability to resist perturbations. Our method is specifically designed for scene editing, possessing the capability to maintain 3D consistency under minor editing perturbations. To demonstrate this, we compare our approach to commonly used generalization models in 8 scenes on the LLFF dataset. Table 1 shows the results of two types of comparisons: one on unedited images with 3D consistency and the other on images with minor editing perturbations that result in some inconsistency. It can be seen that our approach outperforms other models on images with minor inconsistencies resulting from 2D editing, demonstrating our method is more suitable for the 3D scene editing task as shown in Figure 6 that tested in the fern scene on LLFF dataset.

Model efficiency. Since our generalizable model precludes retraining, it is more efficient. A quantitative experiment comparing model efficiency has been incorporated, and the results, as presented in Table 2, show substantial advantages of the proposed DN2N over previous techniques in both runtime and model storage. In terms of runtime, our approach does not require training time for new scenes or new types of edits, only necessitating inference time for editing. Thus, our method is more efficient than alternative techniques. Regarding model storage, our model, which is applicable across all scenes and types of edits, entails a constant space complexity of $O(1)$. In contrast, other methods need to retrain a model for each different scene or type of edit, leading to space complexity of $O(n)$. Thus these methods consume significantly more storage than our model when there are numerous editing scenes or types.

Table 1. **Comparison of PSNR with other generalizable NeRF models on the LLFF dataset.** * indicates that random minor perturbations are applied to the scenes.

	PixelNeRF	MVSNeRF	IBRNet	Neuray	DN2N
LLFF	18.66	21.18	25.17	25.35	23.81
LLFF*	11.03	16.74	20.05	19.31	22.42

Table 2. **Quantitative comparison of time and model size for editing the flower scene in LLFF dataset.** 'TC' and 'SC' stand for Time and Space Complexity, respectively.

	time (minute)			TC	Size(MB)	SC
	train	edit	total			
ARF	21.7	3.4	25.1	O(n)	558	O(n)
DFF	20.6	5.2	25.8	O(n)	144	O(n)
Clip-NeRF	524.4	1034.2	1558.6	O(n)	29.4	O(n)
NeRF-Art	1545.6	780.6	2326.2	O(n)	18.3	O(n)
Instruct-N2N	19.2	62.1	81.3	O(n)	484	O(n)
Ours	0	22.3	22.3	O(n)	103	O(1)

4.3. User study

We perform a user study to evaluate the editing results of DN2N model against state-of-the-art approaches. The study yields 1700 votes in total for three evaluation metrics, that is the 3D consistency, preservation of the original scene content, and the faithfulness to the text description. The vote results are depicted in Figure 7, which shows that the proposed model is favored in terms of these evaluation metrics. The implementation details of the user study can be found in the supplementary materials.

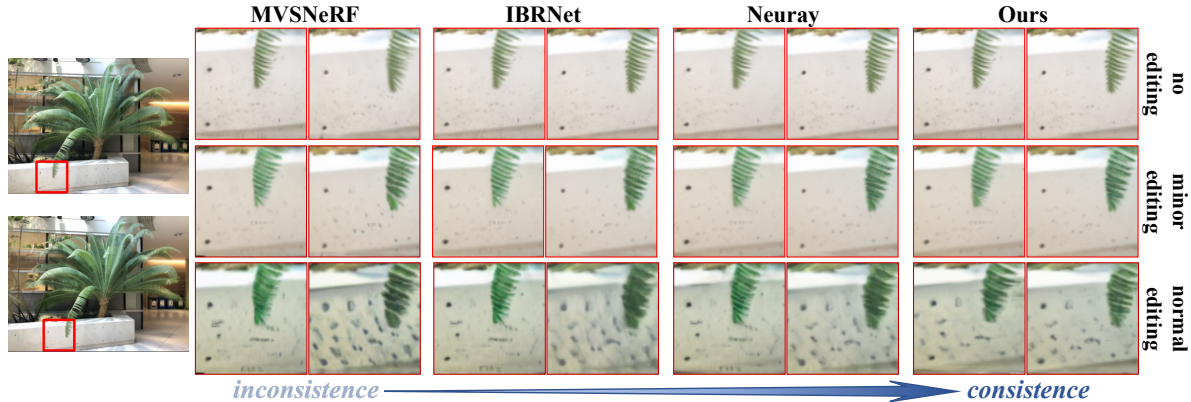


Figure 6. **Comparison with other generalizable models based on NeRF.** Our approach can maintain 3D consistency across novel views under different editing degrees.

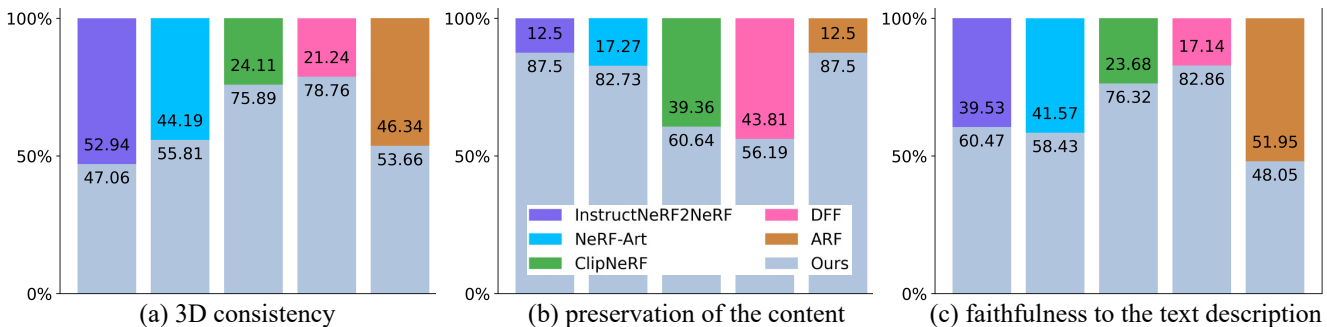


Figure 7. **User study.** The proposed DN2N method performs well against other state-of-the-art approaches in terms of comprehensive performance across three evaluation criteria.

Table 3. **PSNR results of ablation studies.** Experiments are conducted by applying varying minor editing perturbations to the scene in Figure 8. DG denotes data generation.

	w/o DG	w/o l_{self}	w/o l_{nbr}	Full
exp1	17.24	19.89	21.05	21.76
exp2	18.98	21.5	21.92	23.11
exp3	18.73	21.16	22.39	24.21
exp4	18.97	20.53	22.19	22.27

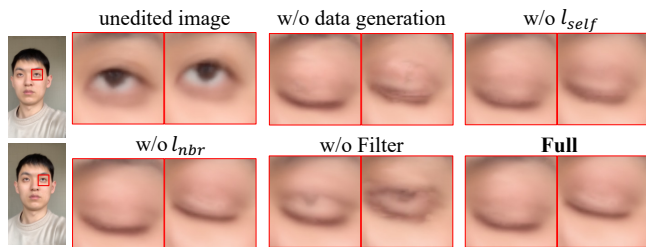


Figure 8. Qualitative ablation studies for key components in editing the ‘open eyes’ to ‘closed eyes’.

4.4. Ablation studies

We demonstrate the contribution of each component in our method in Figure 8. We find that omitting the data generation process during training would significantly affect the model performance on edited results. Furthermore, removing the self and neighboring view components leads to 3D inconsistency. Upon testing the content filter during network inference, we find that its absence results in significant image distortion. This can be attributed to the fact that

editing 2D images directly results in a significant 3D inconsistency between different views, making it difficult for the model to solve these inconsistencies without the content filter. Table 3 shows the quantitative ablation results by assessing the model resistance to disturbance by applying minor perturbations to the scene in Figure 8. It is evident that training the generalization model with perturbed images is crucial. Furthermore, enforcing cross-view consistency can also enhance the model’s overall performance.



Figure 9. **Failed editing case.** The 2D editing model may not always achieve reliable editing results, leading to failures in editing 3D scenes. As in this example, we aim only to edit the color of the leaves in the original image to blue, but both our and the Instruct-NeRF2NeRF methods failed.

4.5. Limitations

Similar to the limitations encountered by the Instruct-NeRF2NeRF method [20], our outcome of the 3D editing is also affected by the 2D image pre-editing process. As illustrated in Figure 9, DN2N does not perform well if the 2D model fails to edit successfully.

5. Conclusion

In this work, we propose a text-driven method for editing 3D scenes that exhibits strong generalization capabilities and enables realistic novel view editing without additional training for each modification task. Our approach leverages existing 2D editing models to perform initial editing of 3D scene data based on textual descriptions. We then filter out poorly edited images and those that disrupt 3D consistency significantly, treating the remaining inconsistency as noise perturbation on top of consistently edited results. To eliminate this perturbation, we provide several approaches to train our model, including creating training data and strengthening cross-view robustness. Our experimental results demonstrate the effectiveness of our approach, which offers significant advantages over conventional methods. Specifically, our method provides greater convenience for editing, supports multiple editing capabilities, and exhibits strong generalization, eliminating the need for training on new scenes and reducing the complexity of the training process and model storage requirements.

References

- [1] Jonathan T Barron, Ben Mildenhall, Matthew Tancik, Peter Hedman, Ricardo Martin-Brualla, and Pratul P Srinivasan. Mip-nerf: A multiscale representation for anti-aliasing neural radiance fields. In *ICCV*, pages 5855–5864, 2021. 2, 3
- [2] Sai Bi, Nima Khademi Kalantari, and Ravi Ramamoorthi. Patch-based optimization for image-based texture mapping. *ACM TOG*, 36(4):106–1, 2017. 3
- [3] Mark Boss, Raphael Braun, Varun Jampani, Jonathan T Barron, Ce Liu, and Hendrik Lensch. Nerf: Neural radiance decomposition from image collections. In *ICCV*, pages 12684–12694, 2021. 3
- [4] Mark Boss, Varun Jampani, Raphael Braun, Ce Liu, Jonathan Barron, and Hendrik Lensch. Neural-pil: Neural pre-integrated lighting for reflectance decomposition. In *NeurIPS*, pages 10691–10704, 2021. 3
- [5] Tim Brooks, Aleksander Holynski, and Alexei A Efros. Instructpix2pix: Learning to follow image editing instructions. *arXiv preprint arXiv:2211.09800*, 2022. 2, 3
- [6] Tom Brown, Benjamin Mann, Nick Ryder, Melanie Subbiah, Jared D Kaplan, Prafulla Dhariwal, Arvind Neelakantan, Pranav Shyam, Girish Sastry, Amanda Askell, et al. Language models are few-shot learners. In *NeurIPS*, pages 1877–1901, 2020. 2, 3, 4, 1
- [7] Tom Brown, Benjamin Mann, Nick Ryder, Melanie Subbiah, Jared D Kaplan, Prafulla Dhariwal, Arvind Neelakantan, Pranav Shyam, Girish Sastry, Amanda Askell, et al. Language models are few-shot learners. In *NeurIPS*, pages 1877–1901, 2020. 3
- [8] Anpei Chen, Zexiang Xu, Fuqiang Zhao, Xiaoshuai Zhang, Fanbo Xiang, Jingyi Yu, and Hao Su. Mvsnerf: Fast generalizable radiance field reconstruction from multi-view stereo. In *ICCV*, pages 14124–14133, 2021. 3
- [9] Anpei Chen, Zexiang Xu, Andreas Geiger, Jingyi Yu, and Hao Su. Tensorf: Tensorial radiance fields. *arXiv preprint arXiv:2203.09517*, 2022. 2, 3
- [10] Pei-Ze Chiang, Meng-Shiun Tsai, Hung-Yu Tseng, Wei-Sheng Lai, and Wei-Chen Chiu. Stylizing 3d scene via implicit representation and hypernetwork. In *IEEE Winter Conference on Applications of Computer Vision*, pages 1475–1484, 2022. 3
- [11] Jooyoung Choi, Sungwon Kim, Yonghyun Jeong, Youngjune Gwon, and Sungroh Yoon. Ilvr: Conditioning method for denoising diffusion probabilistic models. In *ICCV*, pages 14347–14356, 2021. 3
- [12] Prafulla Dhariwal and Alexander Nichol. Diffusion models beat gans on image synthesis. In *NeurIPS*, pages 8780–8794, 2021. 2, 3
- [13] Laura Downs, Anthony Francis, Nate Koenig, Brandon Kinman, Ryan Hickman, Krista Reymann, Thomas B McHugh, and Vincent Vanhoucke. Google scanned objects: A high-quality dataset of 3d scanned household items. In *IEEE In-*

- ternational Conference on Robotics and Automation, pages 2553–2560, 2022. 5
- [14] Shuangkang Fang, Weixin Xu, Heng Wang, Yi Yang, Yufeng Wang, and Shuchang Zhou. One is all: Bridging the gap between neural radiance fields architectures with progressive volume distillation. *arXiv preprint arXiv:2211.15977*, 2022. 2, 3
- [15] Shuangkang Fang, Yufeng Wang, Yi Yang, Weixin Xu, Heng Wang, Wenrui Ding, and Shuchang Zhou. Pvd-al: Progressive volume distillation with active learning for efficient conversion between different nerf architectures. *arXiv preprint arXiv:2304.04012*, 2023. 2, 3
- [16] John Flynn, Michael Broxton, Paul Debevec, Matthew Duvall, Graham Fyffe, Ryan Overbeck, Noah Snavely, and Richard Tucker. Deepview: View synthesis with learned gradient descent. In *CVPR*, pages 2367–2376, 2019. 5
- [17] Sara Fridovich-Keil, Alex Yu, Matthew Tancik, Qinhong Chen, Benjamin Recht, and Angjoo Kanazawa. Plenoxels: Radiance fields without neural networks. In *CVPR*, pages 5501–5510, 2022. 3
- [18] Jiatao Gu, Lingjie Liu, Peng Wang, and Christian Theobalt. Stylenerf: A style-based 3d aware generator for high-resolution image synthesis. In *ICLR*, pages 1–25, 2022. 2, 3
- [19] Fangzhou Han, Shuquan Ye, Mingming He, Menglei Chai, and Jing Liao. Exemplar-based 3d portrait stylization. *IEEE TVCG*, 29(2):1371–1383, 2021. 3
- [20] Ayaan Haque, Matthew Tancik, Alexei A Efros, Aleksander Holynski, and Angjoo Kanazawa. Instruct-nerf2nerf: Editing 3d scenes with instructions. *arXiv preprint arXiv:2303.12789*, 2023. 2, 3, 9
- [21] Kaiming He, Xiangyu Zhang, Shaoqing Ren, and Jian Sun. Deep residual learning for image recognition. In *Proceedings of the IEEE conference on computer vision and pattern recognition*, pages 770–778, 2016. 3
- [22] Amir Hertz, Ron Mokady, Jay Tenenbaum, Kfir Aberman, Yael Pritch, and Daniel Cohen-Or. Prompt-to-prompt image editing with cross attention control. *arXiv preprint arXiv:2208.01626*, 2022. 2, 3
- [23] Jonathan Ho and Tim Salimans. Classifier-free diffusion guidance. *arXiv preprint arXiv:2207.12598*, 2022. 1
- [24] Jonathan Ho, Ajay Jain, and Pieter Abbeel. Denoising diffusion probabilistic models. *Advances in Neural Information Processing Systems*, pages 6840–6851, 2020. 2, 3
- [25] Lukas Höllein, Justin Johnson, and Matthias Nießner. Stylemesh: Style transfer for indoor 3d scene reconstructions. In *CVPR*, pages 6198–6208, 2022. 2, 3
- [26] Fangzhou Hong, Mingyuan Zhang, Liang Pan, Zhongang Cai, Lei Yang, and Ziwei Liu. Avatarclip: Zero-shot text-driven generation and animation of 3d avatars. *arXiv preprint arXiv:2205.08535*, 2022. 3
- [27] Hsin-Ping Huang, Hung-Yu Tseng, Saurabh Saini, Maneesh Singh, and Ming-Hsuan Yang. Learning to stylize novel views. In *ICCV*, pages 13869–13878, 2021. 3
- [28] Yi-Hua Huang, Yue He, Yu-Jie Yuan, Yu-Kun Lai, and Lin Gao. Stylizednerf: consistent 3d scene stylization as stylized nerf via 2d-3d mutual learning. In *CVPR*, pages 18342–18352, 2022. 2, 3
- [29] Mohammad Mahdi Johari, Yann Lepoittevin, and François Fleuret. Geonerf: Generalizing nerf with geometry priors. In *CVPR*, pages 18365–18375, 2022. 3, 4
- [30] Bahjat Kawar, Shiran Zada, Oran Lang, Omer Tov, Huiwen Chang, Tali Dekel, Inbar Mosseri, and Michal Irani. Imagic: Text-based real image editing with diffusion models. *arXiv preprint arXiv:2210.09276*, 2022. 3
- [31] Mijeong Kim, Seonguk Seo, and Bohyung Han. Infonerf: Ray entropy minimization for few-shot neural volume rendering. In *CVPR*, pages 12912–12921, 2022. 5
- [32] Diederik P Kingma and Jimmy Ba. Adam: A method for stochastic optimization. *arXiv preprint arXiv:1412.6980*, 2014. 1
- [33] Sosuke Kobayashi, Eiichi Matsumoto, and Vincent Sitzmann. Decomposing nerf for editing via feature field distillation. *arXiv preprint arXiv:2205.15585*, 2022. 2, 3
- [34] Junnan Li, Dongxu Li, Caiming Xiong, and Steven Hoi. Blip: Bootstrapping language-image pre-training for unified vision-language understanding and generation. In *International Conference on Machine Learning*, pages 12888–12900, 2022. 2
- [35] Junnan Li, Dongxu Li, Silvio Savarese, and Steven Hoi. Blip-2: Bootstrapping language-image pre-training with frozen image encoders and large language models. *arXiv preprint arXiv:2301.12597*, 2023. 2, 3, 4, 1
- [36] Yuan Li, Zhi-Hao Lin, David Forsyth, Jia-Bin Huang, and Shenlong Wang. Climatenerf: Physically-based neural rendering for extreme climate synthesis. *arXiv preprint arXiv:2211.13226*, 2022. 2, 3
- [37] Zhengqin Li, Jia Shi, Sai Bi, Rui Zhu, Kalyan Sunkavalli, Miloš Hašan, Zexiang Xu, Ravi Ramamoorthi, and Manmohan Chandraker. Physically-based editing of indoor scene lighting from a single image. In *ECCV*, pages 555–572, 2022. 3
- [38] Chen-Hsuan Lin, Wei-Chiu Ma, Antonio Torralba, and Simon Lucey. Barf: Bundle-adjusting neural radiance fields. In *ICCV*, pages 5741–5751, 2021. 2, 3
- [39] Lingjie Liu, Jiatao Gu, Kyaw Zaw Lin, Tat-Seng Chua, and Christian Theobalt. Neural sparse voxel fields. In *NeurIPS*, 2020. 2
- [40] Yuan Liu, Sida Peng, Lingjie Liu, Qianqian Wang, Peng Wang, Christian Theobalt, Xiaowei Zhou, and Wenping Wang. Neural rays for occlusion-aware image-based rendering. In *CVPR*, pages 7824–7833, 2022. 3, 4
- [41] Ricardo Martin-Brualla, Noha Radwan, Mehdi SM Sajjadi, Jonathan T Barron, Alexey Dosovitskiy, and Daniel Duckworth. Nerf in the wild: Neural radiance fields for unconstrained photo collections. In *CVPR*, pages 7210–7219, 2021. 2
- [42] Oscar Michel, Roi Bar-On, Richard Liu, Sagie Benaim, and Rana Hanocka. Text2mesh: Text-driven neural stylization for meshes. In *CVPR*, pages 13492–13502, 2022. 3
- [43] Ben Mildenhall, Pratul P Srinivasan, Rodrigo Ortiz-Cayon, Nima Khademi Kalantari, Ravi Ramamoorthi, Ren Ng, and Abhishek Kar. Local light field fusion: Practical view synthesis with prescriptive sampling guidelines. *ACM TOG*, 38(4):1–14, 2019. 5

- [44] Ben Mildenhall, Pratul P Srinivasan, Matthew Tancik, Jonathan T Barron, Ravi Ramamoorthi, and Ren Ng. Nerf: Representing scenes as neural radiance fields for view synthesis. In *ECCV*, pages 405–421, 2020. 2, 3, 5
- [45] Ron Mokady, Amir Hertz, Kfir Aberman, Yael Pritch, and Daniel Cohen-Or. Null-text inversion for editing real images using guided diffusion models. *arXiv preprint arXiv:2211.09794*, 2022. 2, 3, 4, 5, 1
- [46] Fangzhou Mu, Jian Wang, Yicheng Wu, and Yin Li. 3d photo stylization: Learning to generate stylized novel views from a single image. In *CVPR*, pages 16273–16282, 2022. 3
- [47] Fangzhou Mu, Jian Wang, Yicheng Wu, and Yin Li. 3d photo stylization: Learning to generate stylized novel views from a single image. In *CVPR*, pages 16273–16282, 2022. 3
- [48] Thomas Müller, Alex Evans, Christoph Schied, and Alexander Keller. Instant neural graphics primitives with a multi-resolution hash encoding. *arXiv preprint arXiv:2201.05989*, 2022. 2, 3
- [49] Alexander Quinn Nichol, Prafulla Dhariwal, Aditya Ramesh, Pranav Shyam, Pamela Mishkin, Bob McGrew, Ilya Sutskever, and Mark Chen. Glide: Towards photorealistic image generation and editing with text-guided diffusion models. In *International Conference on Machine Learning*, pages 16784–16804, 2022. 3
- [50] Gaurav Parmar, Krishna Kumar Singh, Richard Zhang, Yijun Li, Jingwan Lu, and Jun-Yan Zhu. Zero-shot image-to-image translation. *arXiv preprint arXiv:2302.03027*, 2023. 3
- [51] Adam Paszke, Sam Gross, Francisco Massa, Adam Lerer, James Bradbury, Gregory Chanan, Trevor Killeen, Zeming Lin, Natalia Gimelshein, Luca Antiga, et al. Pytorch: An imperative style, high-performance deep learning library. In *NeurIPS*, 2019. 5, 1
- [52] Aditya Ramesh, Prafulla Dhariwal, Alex Nichol, Casey Chu, and Mark Chen. Hierarchical text-conditional image generation with clip latents. *arXiv preprint arXiv:2204.06125*, 2022. 3
- [53] Robin Rombach, Andreas Blattmann, Dominik Lorenz, Patrick Esser, and Björn Ommer. High-resolution image synthesis with latent diffusion models. In *CVPR*, pages 10684–10695, 2022. 2, 3
- [54] Leonid I Rudin and Stanley Osher. Total variation based image restoration with free local constraints. In *ICIP*, pages 31–35, 1994. 5
- [55] Viktor Rudnev, Mohamed Elgharib, William Smith, Lingjie Liu, Vladislav Golyanik, and Christian Theobalt. Neural radiance fields for outdoor scene relighting. *arXiv preprint arXiv:2112.05140*, 2021. 3
- [56] Chitwan Saharia, William Chan, Saurabh Saxena, Lala Li, Jay Whang, Emily L Denton, Kamyar Ghasemipour, Raphael Gontijo Lopes, Burcu Karagol Ayan, Tim Salimans, et al. Photorealistic text-to-image diffusion models with deep language understanding. In *NeurIPS*, pages 36479–36494, 2022. 2, 3
- [57] Jascha Sohl-Dickstein, Eric Weiss, Niru Maheswaranathan, and Surya Ganguli. Deep unsupervised learning using nonequilibrium thermodynamics. In *International Conference on Machine Learning*, pages 2256–2265, 2015.
- [58] Jiaming Song, Chenlin Meng, and Stefano Ermon. Denoising diffusion implicit models. In *ICLR*, 2021. 2, 1
- [59] Yang Song, Jascha Sohl-Dickstein, Diederik P Kingma, Abhishek Kumar, Stefano Ermon, and Ben Poole. Score-based generative modeling through stochastic differential equations. In *ICLR*, 2021. 3
- [60] Alexey Stomakhin, Craig Schroeder, Lawrence Chai, Joseph Teran, and Andrew Selle. A material point method for snow simulation. *ACM TOG*, 32(4):1–10, 2013. 3
- [61] Matthew Tancik, Vincent Casser, Xinchun Yan, Sabeek Pradhan, Ben Mildenhall, Pratul P Srinivasan, Jonathan T Barron, and Henrik Kretzschmar. Block-nerf: Scalable large scene neural view synthesis. In *CVPR*, pages 8248–8258, 2022. 2
- [62] Jiayang Tang, Xiaokang Chen, Jingbo Wang, and Gang Zeng. Compressible-composable nerf via rank-residual decomposition. *arXiv preprint arXiv:2205.14870*, 2022. 2, 3
- [63] Vadim Tschernezki, Iro Laina, Diane Larlus, and Andrea Vedaldi. Neural feature fusion fields: 3d distillation of self-supervised 2d image representations. *arXiv preprint arXiv:2209.03494*, 2022. 3
- [64] Can Wang, Menglei Chai, Mingming He, Dongdong Chen, and Jing Liao. Clip-nerf: Text-and-image driven manipulation of neural radiance fields. In *CVPR*, pages 3835–3844, 2022. 2
- [65] Can Wang, Ruixiang Jiang, Menglei Chai, Mingming He, Dongdong Chen, and Jing Liao. Nerf-art: Text-driven neural radiance fields stylization. *arXiv preprint arXiv:2212.08070*, 2022. 3, 5
- [66] Qianqian Wang, Zhicheng Wang, Kyle Genova, Pratul P Srinivasan, Howard Zhou, Jonathan T Barron, Ricardo Martin-Brualla, Noah Snavely, and Thomas Funkhouser. Ibrnet: Learning multi-view image-based rendering. In *CVPR*, pages 4690–4699, 2021. 2, 3, 4, 5
- [67] Alex Yu, Ruilong Li, Matthew Tancik, Hao Li, Ren Ng, and Angjoo Kanazawa. Plenotrees for real-time rendering of neural radiance fields. In *ICCV*, pages 5752–5761, 2021. 3
- [68] Kai Zhang, Gernot Riegler, Noah Snavely, and Vladlen Koltun. Nerf++: Analyzing and improving neural radiance fields. *arXiv preprint arXiv:2010.07492*, 2020. 2
- [69] Kai Zhang, Nick Kolkin, Sai Bi, Fujun Luan, Zexiang Xu, Eli Shechtman, and Noah Snavely. Arf: Artistic radiance fields. In *ECCV*, pages 717–733, 2022. 2, 3
- [70] Qian-Yi Zhou and Vladlen Koltun. Color map optimization for 3d reconstruction with consumer depth cameras. *ACM TOG*, 33(4):1–10, 2014. 3

Text-driven Editing of 3D Scenes without Retraining

Supplementary Material

6. Background of neural radiance fields and diffusion models.

Neural radiance fields. NeRF utilizes an implicit function to represent scenes, which maps the spatial point $\mathbf{x} = (x, y, z)$ and view direction $\mathbf{d} = (\theta, \phi)$ to the density σ and color \mathbf{c} . Typically, the implicit function is represented by an MLP network, denoted as $F_{\Theta} : (\mathbf{x}, \mathbf{d}) \rightarrow (\sigma, \mathbf{c})$, where Θ represents the weights of the network. For a ray \mathbf{r} originating at \mathbf{o} with direction \mathbf{d} , the RGB value $\hat{\mathbf{C}}(\mathbf{r})$ of the corresponding pixel is estimated through numerical quadrature of the color \mathbf{c}_i and density σ_i of the spatial points sampled along the ray:

$$\hat{\mathbf{C}}(\mathbf{r}) = \sum_i^N T_i (1 - \exp(-\sigma_i \delta_i)) \mathbf{c}_i, \quad (10)$$

where N is the number of sample points, δ_i denotes the distance between adjacent sample points, and $T_i = \exp(-\sum_{j=1}^{i-1} \sigma_j \delta_j)$. Here $T_i (1 - \exp(-\sigma_i \delta_i))$ is used to calculate the entropy loss as defined in Eq. 7 in the main text.

Text-guided diffusion models. Text-guided diffusion models aim to generate an output image z_0 from a random noise vector z_t under a textual condition \mathcal{P} . To achieve sequential denoising, the model ε_{θ} is trained to predict artificial noise, minimizing the objective:

$$\min_{\theta} E_{z_0, \varepsilon \sim N(0, I), t \sim \text{Uniform}(1, T)} \|\varepsilon - \varepsilon_{\theta}(z_t, t, \mathcal{C})\|_2^2, \quad (11)$$

where $\mathcal{C} = \psi(\mathcal{P})$ denotes the embedding of the text condition, and z_t is a noised sample according to the timestamp t . During the inference process, given a noise vector z_T , its noise is gradually removed by sequential prediction using a trained network for T steps, which can be achieved by the DDIM sampling strategy [58]. Amplifying the effect induced by the conditioned text is a significant challenge in a text-guided generation. To address this issue, Ho et al. [23] propose a guidance technique that eliminates the need for a classifier in unconditional prediction and extends it to conditioned prediction scenarios. With the introduced concept of a null text embedding, denoted as $\emptyset = \psi(\text{""})$, and a guidance scale parameter w , then the guidance prediction is given by:

$$\tilde{\varepsilon}_{\theta}(z_t, t, \mathcal{C}, \emptyset) = w \cdot \varepsilon_{\theta}(z_t, t, \mathcal{C}) + (1-w) \cdot \varepsilon_{\theta}(z_t, t, \emptyset). \quad (12)$$

In our experiments, we primarily control the degree of image editing by adjusting the parameter guidance scale parameter w and inversion steps T .

7. Additional implementation details

7.1. Process of generating training data

Generate input and target captions. During the training phase, we utilized a total of 1246 3D scenes. For each scene, we randomly select one image to generate an input caption using the BLIP-2 model [35] with 2.7 billion parameters¹. A subset of the generated captions is shown in Figure 10. After obtaining the input captions for each scene, we utilize the GPT model [6] to generate target captions. To be specific, we prompt GPT to provide a list of 100 renowned painters, 100 paintings, and 50 painting schools. Afterward, we randomly combine the input captions with the content generated by GPT, following a fixed template, to generate target captions pertaining to style transfer. For other types of editing, we instruct GPT to add, delete, or replace words in the input captions. The prompts and several generated samples are shown in Table 4.

Minor perturbations for training. We generate the training data by applying minor random perturbations to the 3D scene using the Null-text [45] 2D editing model². The random ranges for the relevant parameters are set as follows: 100 to 300 for the iteration number T and 0.5 to 3.5 for the text guidance scale w .

Normal perturbations for inference. For normal-scale edits, we follow the recommended settings from the Null-Text paper, with $w=7.5$ and $T=500$.

The effects of applying random minor perturbations and normal editing to the images are depicted in Figure 11.

7.2. Training and inference

Training phase. In the training process, the input caption for the current scene can be directly retrieved from a pre-stored file. As for the target caption, it is generated randomly based on Table 4. To be specific, we employ a weight of 2:2:2:4 to randomly choose one column from the four columns in Table 4 and then select its target caption for the current scene.

Our method is implemented using the PyTorch framework [51]. We employ the Adam optimizer [32] with initial learning rates of $1e-4$ for the CNN and $5e-4$ for the MLP. The training process runs for 300K steps with a batch size of 500 rays. The initial values for the loss weight in Eq. 8 in the main text of l_{self} , l_{nbr} , l_{en} , and l_{tv} , are set as $\lambda_1=1e-3$, $\lambda_2=1e-3$, $\lambda_3=1e-3$, and $\lambda_4=2e-3$, respectively. The calculation of l_{nbr} is only performed after the iteration count ex-

¹<https://huggingface.co/Salesforce/blip2-opt-2.7b>

²<https://null-text-inversion.github.io>



Figure 10. **Generate input captions by BLIP.** For each 3D scene, we randomly select one image to generate its input caption using the BLIP-2 model.

Table 4. **Generate target captions by GPT.** Given the input caption **S** for a 3D scene, we utilize GPT to generate a target caption **O**. For instance, if **S** is 'yellow roses in the garden', the target captions can be 'Leonardo da Vinci painting of yellow roses in the garden', 'yellow roses in the garden in the Rococo style', 'pink roses in the garden', to name a few.

Prompts	List 100 famous painters	List 50 famous painting schools	List 100 famous paintings	Replace, add or delete partial words in the following sentences: S ₁ , S ₂ , ...
GPT outputs (O)	Leonardo da Vinci Vincent van Gogh Pablo Picasso Sam Francis Max Ernst ⋮	Baroque Realism Impressionism Op Art Fauvism ⋮	Mona Lisa The Last Supper The Scream The Starry Night Guernica ⋮	pink roses in the garden red roses in the garden white roses in the garden orange roses in the garden purple roses in the garden ⋮
	Henri Matisse Eva Hesse Carl Andre Cy Twombly Jan van Eyck	Tonalism Ashcan School Rococo Symbolism Outsider Art	The Fifer The Kiss The Hay Wagon Olympia Sunflowers	a green couch with gold trim a green chair with silver trim a green chair with no trim a blue chair with gold trim a white chair with gold paint
Target captions	O painting of S or S in the O style	O painting of S or S in the O style	S in the O style	O

ceeds 10K. During the training phase, we randomly select a variable number of source views ranging from 6 to 15, while using 15 source views during inference. The number of sampled points on a ray is set to 64.

Inference phase. After completing the training process, given a scene and its corresponding textual description, we apply normal-level editing to the images of the scene using

the 2D editing model. Following that, we employ a content filter to select the edited results, removing the lowest and highest 10% of values for each of the four metrics defined in Eq. 9 in the main text.

Implementation details of the content filter. The main idea behind the content filter is to maintain the degree of editing consistent across various perspectives. To achieve

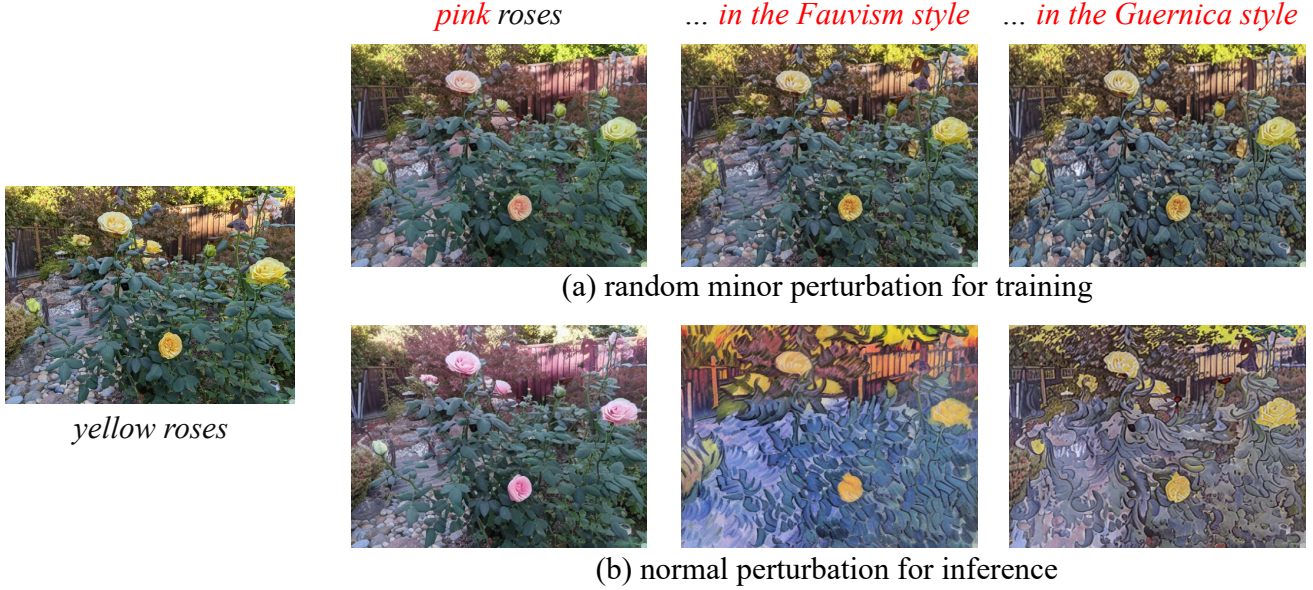


Figure 11. **Visualization of random minor perturbations and normal perturbations.** After applying 2D editing to the scene, the images exhibit various types of distortions in color or structure, thereby compromising the consistency among them. To simulate this 3D inconsistency, we introduce minor perturbations to the clean scene and optimize our model to remove them.

this, we consider the following two situations:

(1). A smaller degree of editing implies fewer changes in the edited image relative to the original, while a larger discrepancy with the target text. (2). Conversely, a higher degree of editing denotes more significant changes in the edited image compared to the original, bringing it closer to the target text.

Therefore, the evaluation metrics used in the content filter can be measured through the relationship between the original image, edited image, original text description, and target text description. Specifically, given an original image I_i and its caption C_{in} , as well as its corresponding edited image \tilde{I}_i and its caption C_{tgt} , we calculate the following four measurements based on SSIM similarity and CLIP similarity during the filtering process: (a): $SSIM(I_i, \tilde{I}_i)$, (b): $CLIP(I_i, \tilde{I}_i)$, (c): $CLIP(\tilde{I}_i, C_{tgt})$, (d): $CLIP(I_i, \tilde{I}_i) - CLIP(C_{in} - C_{tgt})$.

Here, the metrics (a) and (b) assess the similarity between the image before and after editing. The metric (c) gauges the similarity between the edited image and the target caption, while the metric (d) evaluates the relative offset between the text and the image. These indicators assess the editing results on different dimensions. The role of our content filter is to eliminate extreme values (top 10% and bottom 10% of them) from these metrics, ensuring that the remaining images tend toward consistent editing results.

In Figure 12, we provide the maximum, minimum, and median values for each of the aforementioned metrics, along with their corresponding original and edited images.

Figure 12 shows that the editing results with maximal and minimal metric values exhibit larger image discrepancies. These will pose greater challenges for subsequent 3D consistency. Our content filter, by eliminating these extreme editing results, facilitates superior 3D editing outcomes.

8. Network architecture

Initially, we utilize a UNet-like network with the ResNet34 [21] backbone to extract features from both the unedited and edited source views. These feature maps are then concatenated and inputted into subsequent CNN networks to derive the final feature maps. When estimating the color c and density σ of sampled points along the rays, we primarily employ the MLP networks to integrate, extract, and interpret information from the edited images, feature maps, and viewing directions. For density prediction, we adopt a design of transformer networks inspired by IBR-Net [66]. Regarding the color estimation, we incorporate additional pixel difference information among source views to capture the extent of editing across different perspectives, aiding the network in improved learning. The detailed network architecture and data propagation process are depicted in Figure 13.

9. Additional ablation studies

In this section, we present additional visualization and ablation experiments related to the self-view (l_{self}) and neighboring-view (l_{nbr}) regularization terms. Specifically,

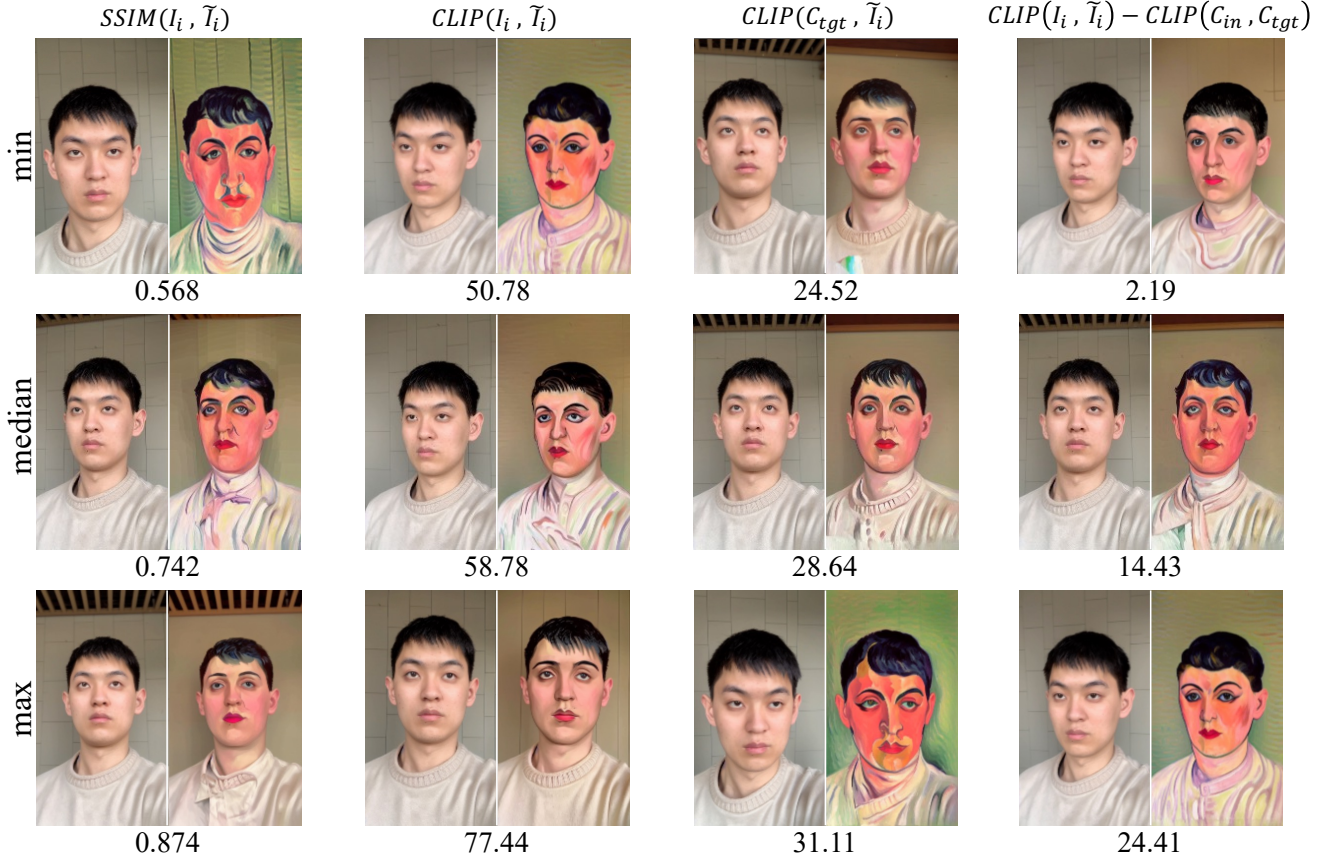


Figure 12. **Visualization of filtered images.** In the figure, we present the edited images corresponding to the maximum and minimum values of each term in Eq. 9 in the main text. These images often exhibit either low or excessive editing degrees. By excluding them, we can enhance the 3D consistency among the remaining images.

we edit the flower scene in the LLFF dataset to a transparent ice sculpture flower. During this editing experiment, we visualize the results obtained by rendering with different source views and the rendering results of different neighboring views. The results are shown in Figure 14 and Figure 15. It can be observed that there is poor 3D consistency and varying degrees of color distortion in the results rendered under different source views. While after incorporating our designed l_{self} regularization term, this phenomenon is significantly alleviated. Similarly, there is a slight inconsistency among the results from different neighboring views, which is improved by introducing the l_{nbr} regularization term.

10. User study details

We invited a total of 50 subjects (31 males and 19 females, aged 18 to 45) to participate in the user study. Each participant is presented with videos or frames generated by various methods. They are asked to select their preferred option based on three distinct criteria: 3D consistency, content

preservation, and faithfulness to the text description. The user study compared our method to others across 4 scenes with 18 questions. We use 23 videos to evaluate 3D consistency in 9 questions, and 24 images in the remaining 9 questions to measure the match between text prompts, editing results, and original image content preservation. Typical questions in the questionnaire are:

- (1). What is the video with higher consistency?
- (2). Please select an image that retains more of the original image content.
- (3). Please select an image that more closely matches the text "Elf."

A screenshot of the questionnaire is available in Figure 16.

11. Visualization of geometric information

We visualize the depth maps before and after scene editing, as shown in Figure 17. This is divided into two cases: first, when only appearance is edited, the depth maps before and after exhibit negligible differences. Second, for edits alter-

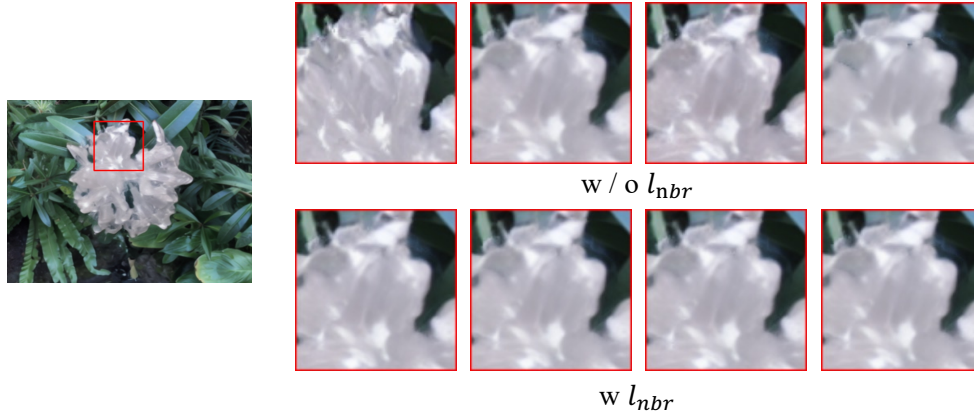
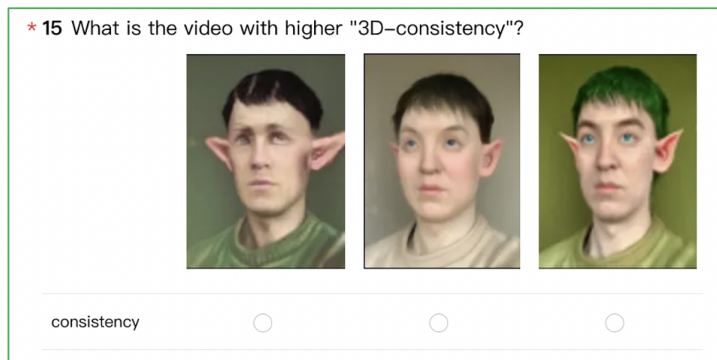
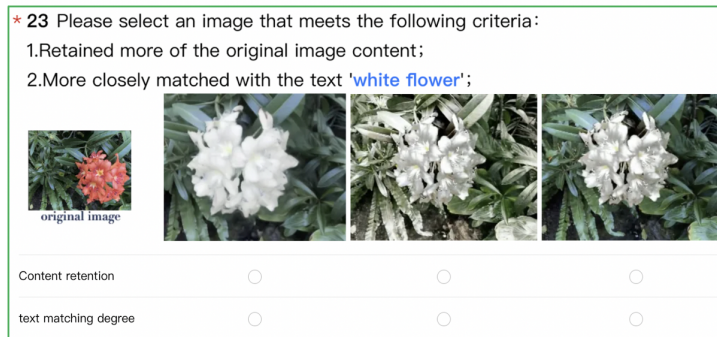


Figure 15. **Ablation study on l_{nbr} regularization term.** A slight inconsistency exists among the results obtained from different neighboring views, which can be mitigated by introducing the l_{nbr} regularization term.



(a) Example of the user study on 3D consistency.



(b) Example of the user study on the content retention and text-image matching degree.

Figure 16. **Example of questionnaire for user study.**

ing the geometry of objects, the depth maps correspondingly exhibit changes as well, validating the 3D awareness of our editing approach.

12. Additional editing results

In this section, we present a collection of additional editing results that showcase the remarkable editing capabilities

and effects of our method. The results are shown as Figure 18, Figure 19 and Figure 20. Additionally, in Figure 21, we delve into more complex cascaded editing scenarios. Even after multiple rounds of editing on the scenes, our method maintains the 3D consistency among novel views and effectively preserves the original scene content.

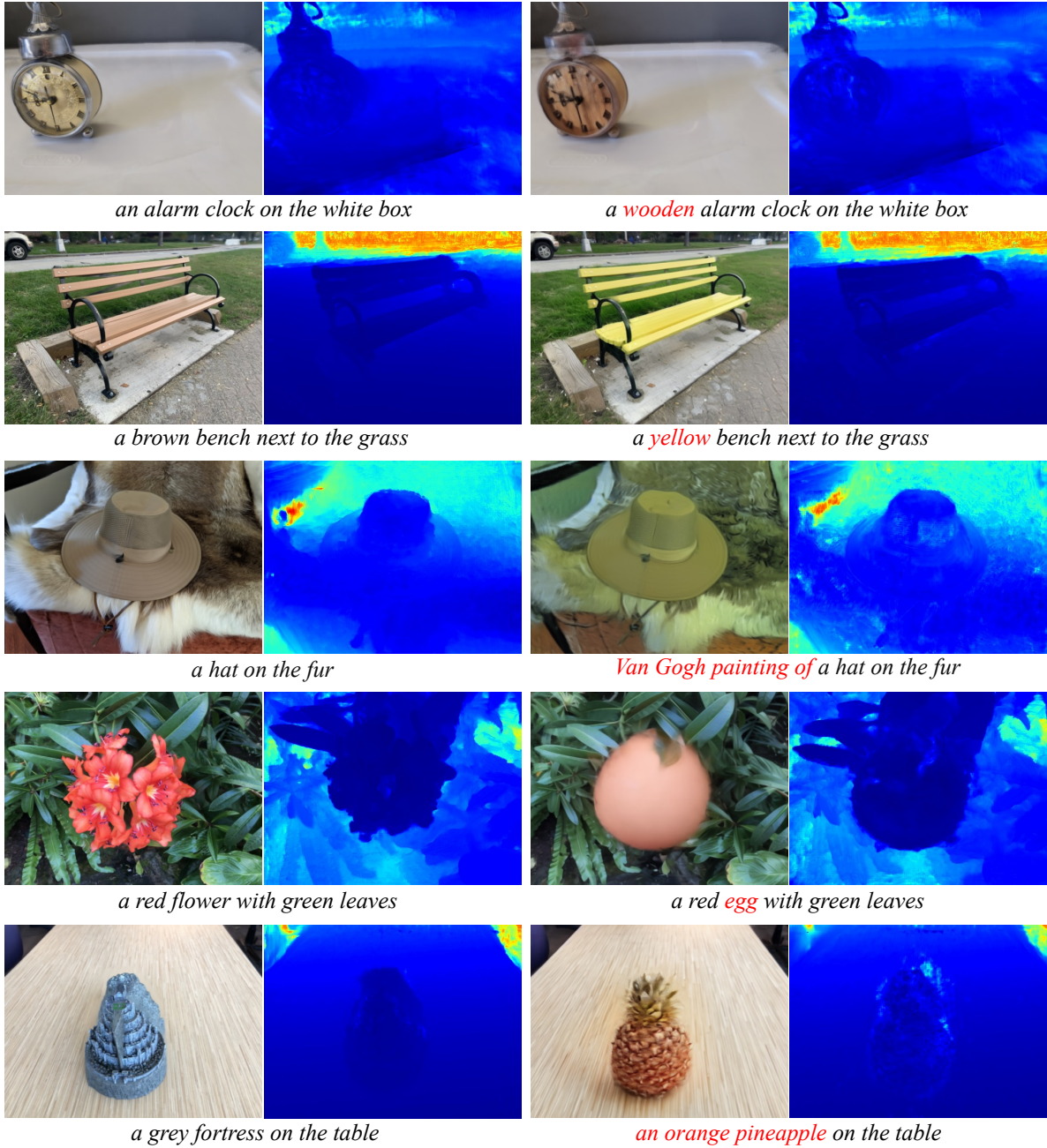


Figure 17. Visualization of geometric information.



a red flower with green leaves



a azure flower...



a milky-white flower...



...leaves covered with snow



... leaves in the heavy rain



a red origami flower...



a transparent ice sculpture flower...



...leaves in the ink and wash style



Modigliani painting of a red...

Figure 18. More visual results on flower editing.



a man is in front of the wall



a golden man sculpture is in front of the wall



a wood man sculpture is in front of the wall



a silver man sculpture is in front of the wall



a man with yellow hair is in front of the wall



a woman is in front of the wall



a child is in front of the wall



an old man is in front of the wall



a saiyan is in front of the wall



a man with closed eyes is in front of the wall



a man with glasses is in front of the wall



a man with suit is in front of the wall



The Tolkien Elf is in front of the wall

Figure 19. More visual results on portrait editing.



a group of green leaves



Van Gogh painting of...



Expressionism painting of...



Paul Gauguin painting of...



... in the Rembrandt style



... in the Op Art style



Mark Rothko painting of...



...in The Slave Ship style



Wassily Kandinsky painting of...



... in the Surrealism style



...in Der Kuss style



... in the Henri Matisse style



Jackson Pollock painting of ...

Figure 20. More visual results on style editing.

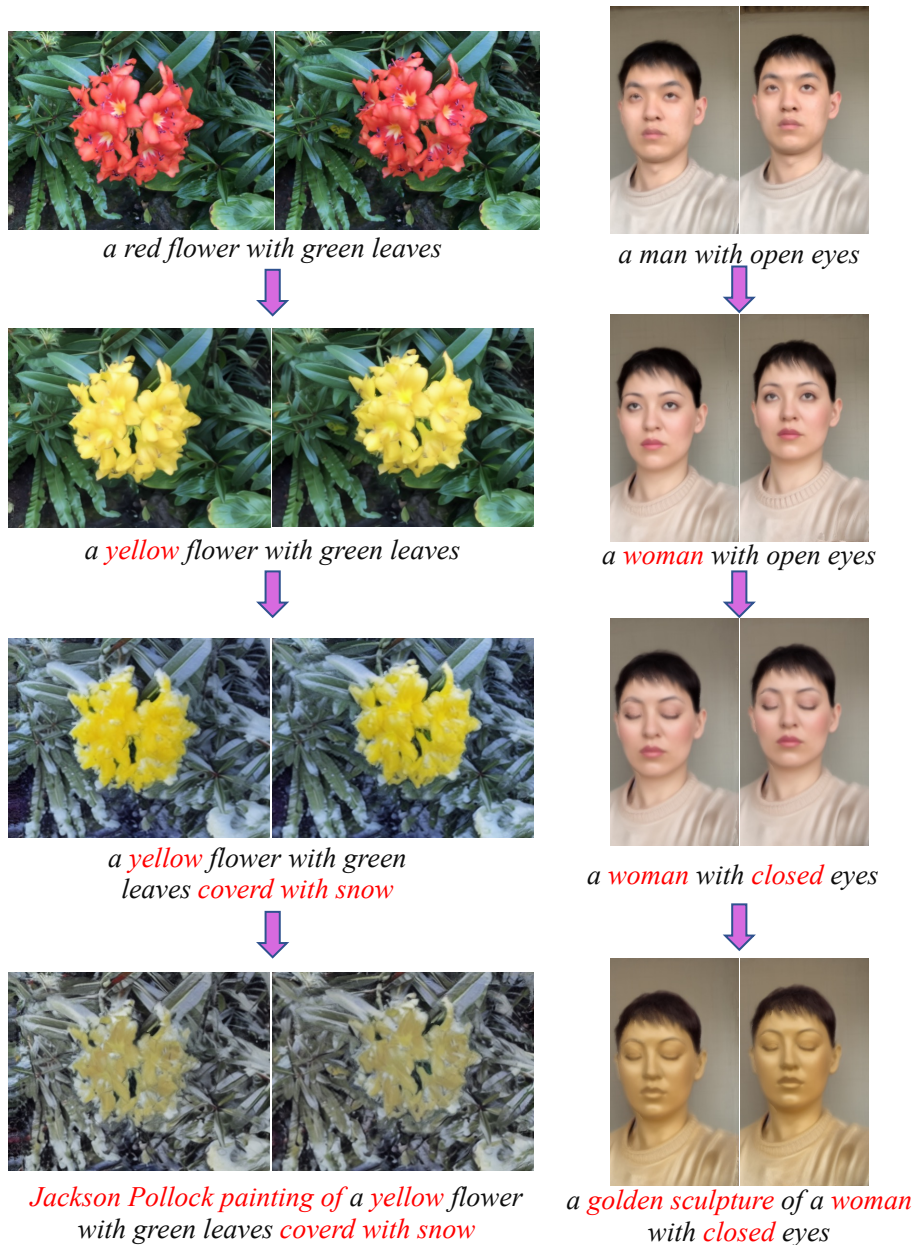


Figure 21. **Cascade editing results.** We begin by applying an edit to the original scene, and then generate a new scene with the desired editing effect using DN2N. We repeat this process by applying another edit to the new scene. In this figure, we showcase the consecutive results of three cascaded editing.